Presented at the Flemings Symposium, Boston, MA, June 2000

# MODELING OF MACROSEGREGATION: PAST, PRESENT AND FUTURE

Christoph Beckermann

Department of Mechanical Engineering
University of Iowa
Iowa City, IA 52242

## Abstract

Modeling of macrosegregation has experienced explosive growth since the pioneering studies of Flemings and coworkers in the mid-1960s. This article presents a review of early contributions, followed by several examples of more recent studies where generalized versions of Flemings' macrosegregation model have been applied to industrial casting processes. The successes and shortfalls of the models in predicting measured macrosegregation patterns are highlighted. Next, advanced macrosegregation models that include a detailed consideration of the solidification microstructure are reviewed. Model results are presented that illustrate the profound effects of combined solid movement and melt convection on macrosegregation. Important issues deserving future research attention are identified.

## Introduction

Modeling of macrosegregation in metal alloy castings is one of the areas in which Professor Merton C. Flemings of MIT made the key contributions in the 1960s that have defined the field for subsequent generations of researchers. Flemings and coworkers discovered the importance of convection within the mushy zones of solidifying alloys and derived the basic equation describing macrosegregation due to interdendritic flow. Over the years, this research has led to numerous improvements in industrial casting processes, and even a better understanding of convection in the mushy zones of the Earth's core, solidifying magmas, and sea ice. Modeling of macrosegregation is still a very active research field, motivated by the fact that producers of virtually all types of cast metals continue to struggle with macrosegregation defects. The rejection of single-crystal superalloy turbine blades due to the presence of freckles is only one of the more pressing examples. The phenomena involved in alloy solidification that lead to macrosegregation are so complex that their quantitative prediction for industrially relevant casting processes is only beginning.

The purpose of this article is not only to review the early contributions of Flemings in this field, but also to provide a brief summary of the developments since then and an outlook of where the field is going. Recent and more detailed reviews of macrosegregation modeling are available in the literature [1-3]. The keynote address given by Flemings at the most recent Modeling of Casting, Welding and Advanced Solidification Processes Conference [4] also contains a historical perspective of macrosegregation modeling. An examination of the proceedings of that conference will show that macrosegregation is the area with the second largest number of contributed papers (after modeling of mold filling), further attesting to the vigorous current activities in this field.

Before proceeding, it is useful to recall that the cause of macrosegregation is the long-range advection of alloy species due to the relative movement or flow of segregated liquid and solid during solidification. There are numerous causes of fluid flow and solid movement in casting processes:

- flow that feeds the solidification shrinkage and the contractions of the liquid and solid during cooling;
- buoyancy induced flows due to thermal and solutal gradients in the liquid; the thermal and solutal buoyancy forces can either aid or oppose each other, depending on the direction of the thermal gradient and whether the rejected solutes cause an increase or a decrease in the density of the liquid;

- forced flows due to pouring, motion of gas bubbles, applied magnetic fields, stirring, rotation, vibration, etc.;
- movement of free (equiaxed) grains or solid fragments that have heterogeneously nucleated in the melt, separated from a mold wall or free surface, or melted off of dendrites; the solid can either float or settle depending on its density relative to the liquid;
- deformation of the solid network due to thermal stresses, metallostatic head, shrinkage stresses, or external forces on the solid shell such as those from the rolls in continuous casting of steel.

All efforts to prevent macrosegregation are aimed at controlling fluid flow and solid movement. Examples include adjustments to the alloy composition or thermal gradients to induce a stable density stratification in the liquid; application of nozzles, baffles, porous materials, centrifugal forces, or electromagnetic fields to redistribute the flow; changes in the riser or mold design to influence the cooling and thermal convection patterns; addition of inert particles (as in composites) to change the effective viscosity of the melt; controlled deformation such as soft reduction during continuous casting of steel to squeeze highly enriched liquid away from the centerline of slabs; and modifications to the grain structure (e.g., grain refiners) that change the resistance to flow through the solid network or the prevalence of equiaxed grains.

Macrosegregation models are generally aimed at understanding the basic mechanisms involved, quantitatively predicting the occurrence and severity of macrosegregation, and performing parametric studies for control and improvement of casting processes. Such models are very complex and require large computing resources in their solutions, because they often must consider many aspects of a solidification process simultaneously. Phenomena to be considered include heat transfer, solute transport, fluid flow, solid movement, and deformation at the (macroscopic) scale of the casting, as well as phase equilibrium, nucleation, structure formation, segregation, and flow at various microscopic scales. Any factors that affect the flow and the microstructure also influence macrosegregation, and vice versa. Figure 1 illustrates many of these interactions in casting processes. Today, it is certainly not desirable to generate a macrosegregation model that includes all of the effects listed in Figure 1, since a model of such complexity would hardly be useful in practice. Consequently, this article focuses on examples of research where *some* of these interactions are taken into account in order to address industrially relevant macrosegregation problems.

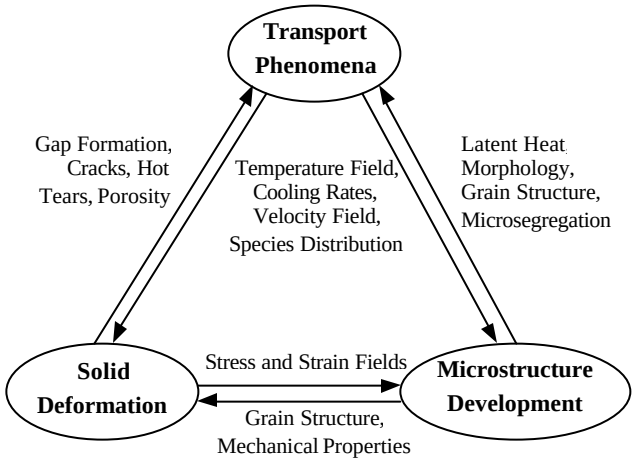


Figure 1: Potentially important interactions in modeling macrosegregation in castings.

Work by Flemings and Coworkers up to the early 1980s

The macrosegregation model developed by Flemings et al. in the latter half of the 1960s [5-7] considered the flow of interdendritic liquid through a fixed dendritic solid network, as shown in Figure 2 [4]. Flow in the all liquid region and movement or deformation of solid were not treated explicitly. By performing mass and species balances on the "mush" volume element in Figure 2, while accounting for possible in/outflow of liquid and the different densities of the two phases, Flemings et al. derived the following "local solute redistribution equation" (LSRE):

$$\frac{df_l}{dC_l} = -\frac{(1-ß)}{(1-k)}\left[1+\frac{\mathbf{v}\cdot\nabla T}{\varepsilon}\right]\frac{f_l}{C_l} \qquad (1)$$

where $f_l$ is the liquid fraction; $C_l$ is the solute concentration in the liquid; $ß = (\rho_s-\rho_l)/\rho_s$ is the solidification shrinkage, in which $\rho_l$ and $\rho_s$ are the densities of the liquid and solid, respectively; $k$ is the partition coefficient; $\mathbf{v}$ is the velocity vector of the liquid; $\nabla T$ is the temperature gradient; and $\varepsilon$ is the rate of temperature change.

The physical significance of Eq. (1) can be understood as follows (for $k$<1):

1. Equation (1) reduces to the Scheil equation, implying no macrosegregation, when $ß$ and $\mathbf{v}$ both vanish.
2. Equation (1) also reduces to the Scheil equation when the

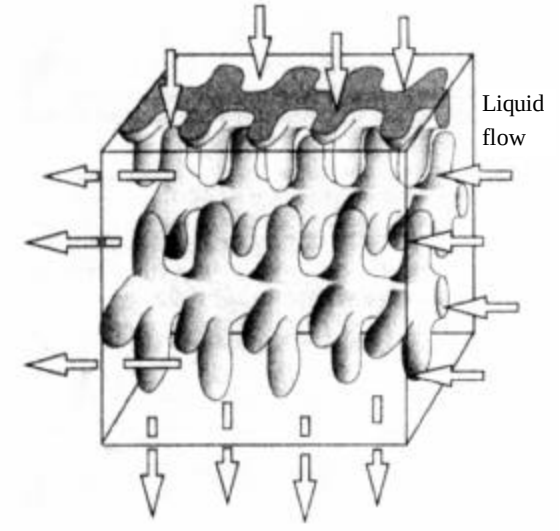


Figure 2: Schematic of interdendritic liquid flow through a fixed dendritic solid network (courtesy of M.C. Flemings, MIT).

liquid velocity is just that required to feed solidification shrinkage.

3. If the liquid velocity alone is zero, for example at an impenetrable chill face, but the shrinkage ß is finite (>0), positive macrosegregation results – this is the so-called inverse segregation often observed in casting of aluminum alloys.
4. Flow in the same direction as the shrinkage flow (i.e., in the direction of decreasing temperature), but with a speed *greater* than the shrinkage velocity, results in negative macrosegregation.
5. Flow in the same direction as the shrinkage flow, but with a speed *less* than the shrinkage velocity, and flow that is in the opposite direction (in the direction of increasing temperature, towards regions of lower solid fraction), results in positive macrosegregation. Examples include centerline and under-riser segregation in steel casting.
6. If the flow velocity in the direction of increasing temperature is so large that the term in the square brackets in Eq. (1) becomes negative, local melting results. This is the cause of the open channels in the mush that lead to A-segregates or freckles.

Mehrabian et al. [8] proposed that the interdendritic flow velocities could be calculated from Darcy's law for flow in porous media:

$$\mathbf{v} = -\frac{K}{\mu f_l}\left(\nabla P + ?_l \boldsymbol{g}\right) \qquad (2)$$

where $K$ is the permeability; $\mu$ is the viscosity; $\nabla P$ is the pressure gradient; and $\boldsymbol{g}$ is the gravity vector. Piwonka and Flemings [9] and Apelian et al. [10] were the first researchers to perform experiments to measure the permeability of mushy zones as a function of the liquid fraction and microstructural parameters, such as the dendrite arm spacings.

Flemings et al. applied the above model to various alloys and casting situations in order to predict typical macrosegregation patterns and verify them experimentally. For example, Mehrabian et al. [11] predicted the conditions for freckling, and Kou et al. [12] predicted the conditions for rotating, axisymmetric ingots. Early work by Mehrabian and Flemings [13] on ternary alloys was extended in the late 1970s by Fujii et al. [14] to macrosegregation in multicomponent low-alloy steel. Fujii et al. solved the coupled LSRE and Darcy's law, but the temperature field was taken from measurements. A shortcoming of all of the above studies is the neglect of the flow in the (fully melted) bulk liquid region ahead of the mushy zone.

The first macrosegregation model that accounted for the coupling of the flow between the mushy and bulk liquid zones was reported by Ridder et al. [15] in 1981. They solved the coupled Darcy's law, energy equation, and LSRE in the mushy zone and the momentum and energy equations in the fully liquid region. Solutal convection in the bulk liquid was neglected. Predicted macrosegregation patterns compared favorably with experimental measurements. In the numerical solution of the equations, a two-domain approach was employed where boundary conditions were explicitly satisfied at the boundary between the mushy and bulk liquid zones and each region was meshed separately. Because they considered a quasi-steady system, the grid did not evolve with time.

Single-Domain Models

Inspired by the work of Flemings et al., as well as by other theoretical work in the early 1980s [16-18], Bennon and Incropera [19] and Beckermann and Viskanta [20] derived continuum or volume-averaged models for macrosegregation in alloy solidification in the mid-1980s at Purdue University. Other early investigators pursuing the same ideas include Voller et al. [21] and Poirier and et al. [22, 23]. These models consist of a set of momentum, energy, and solute conservation equations that are equally valid in the solid, mushy, and liquid regions of solidification systems. Hence, the equations can be solved using a single-domain, fixed numerical grid. The LSRE of Flemings et al., Eq. (1), can be derived from the single-domain models as a limiting case. The momentum equations are a generalization of Darcy's law, Eq. (2), and reduce to the single-phase Navier-Stokes equations in the liquid region. The numerical results obtained in these studies illustrate the importance of coupling the flow between the mushy and liquid zones, and reveal the existence of complex thermo-solutal convection patterns in the melt. In particular, Bennon and Incropera [24] presented the first direct numerical simulations of freckles or A-segregates.

Single-domain continuum or volume-averaged models have been further developed and used by numerous researchers. The articles by Prescott and Incropera [2] and Combeau et al. [3] thoroughly review the very substantial body of literature on this subject, including experimental validation. Another review by Worster [25] illustrates the strong interest of the fluid-mechanics community in the same subject. Instead of providing another comprehensive summary of this research, the remainder of this section is devoted to presenting four applications of single-domain macrosegregation models to industrially relevant casting processes. These examples are intended to illustrate the present state-of-the-art in macrosegregation modeling and to highlight some of its shortcomings. In all four examples, the models assume a fixed, rigid solid in the mush.

*Example 1: Steel Ingot*

The first example involves the prediction of the classical macrosegregation pattern in heavy steel ingots [26], as shown schematically in Fig. 3. The model utilized in this work [27] considers all alloying elements in the steel, including their different segregation behaviors and effects on the liquid density. The mold geometry and thermal boundary conditions were patterned after an experimental ingot cast at Lukens Steel Company. Results for the predicted evolution of the solid fraction and liquid velocity distributions are shown in Fig. 4 for four different times. Strong buoyancy driven flow persists throughout the solidification process. Measured and predicted macrosegregation profiles at the vertical ingot centerline are compared in Fig. 5 for carbon and sulfur. While the level and variation of the macrosegregation are generally predicted well, the pickup of carbon from the insulation material leads to an underprediction of the measured positive carbon macrosegregation near the very top; no such disagreement exists for sulfur. The neglect of the movement of equiaxed crystals in the model prevents the prediction of V-segregates and, perhaps, the measured negative macrosegregation in the bottom half of the ingot; it also leads to a corresponding underprediction of the positive macrosegregation near the hot top junction. Not shown here is the fact that the model also failed to predict the off-

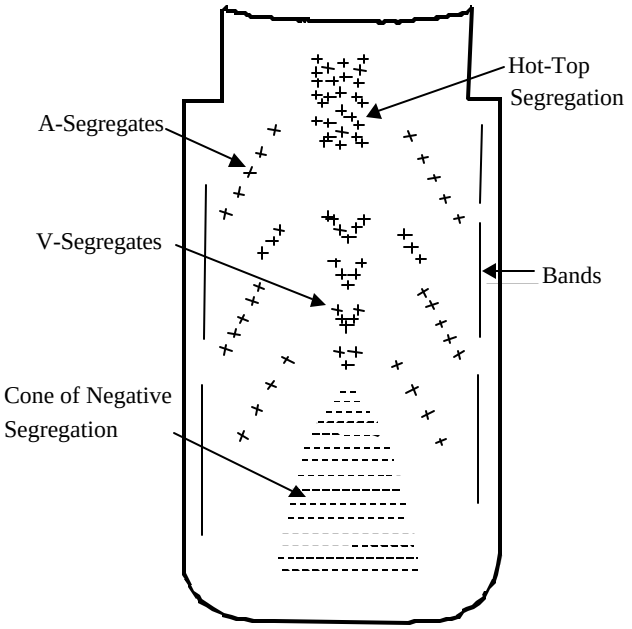


Figure 3: Schematic of the macrosegregation pattern in a steel ingot (after Flemings [26]).

centerline A-segregates (see Fig. 3) observed in the experimental ingot. This can be directly attributed to the coarse numerical grid used in the simulations. An earlier numerical study using the same model with a finer grid for a smaller domain readily predicted A-segregates for a low-alloy steel [28]. In summary, this study revealed a number of shortcomings in macrosegregation modeling for a large steel ingot that are not easily overcome. Even if the model was to be extended to include the generation, growth and settling of equiaxed grains, the computational resources required to resolve flow patterns associated with A-segregates (i.e., on a scale of a few millimeters) over an ingot about 2.5 meters tall and solidifying over more than 10 hours probably will be unavailable for at least the next decade.

*Example 2: Aluminum DC-Casting*

The next example deals with macrosegregation in DC-casting of aluminum alloys. At the Alcoa Technical Center, Finn et al. [29] cast experimental Al-4.5 wt% Cu cylindrical ingots both with and without grain refiner, as schematically illustrated in Fig. 6a. They concluded that for the grain-refined ingot, the mushy zone is *more* permeable and allows for advection, by buoyancy-driven flow, of solute-rich liquid toward the centerline, producing *positive* macrosegregation there. On the other hand, the *less* permeable mush, in the case without grain refiner, reduces such advection, and the remaining shrinkage-driven flow produces *negative* centerline segregation. In both cases, strong positive macro-

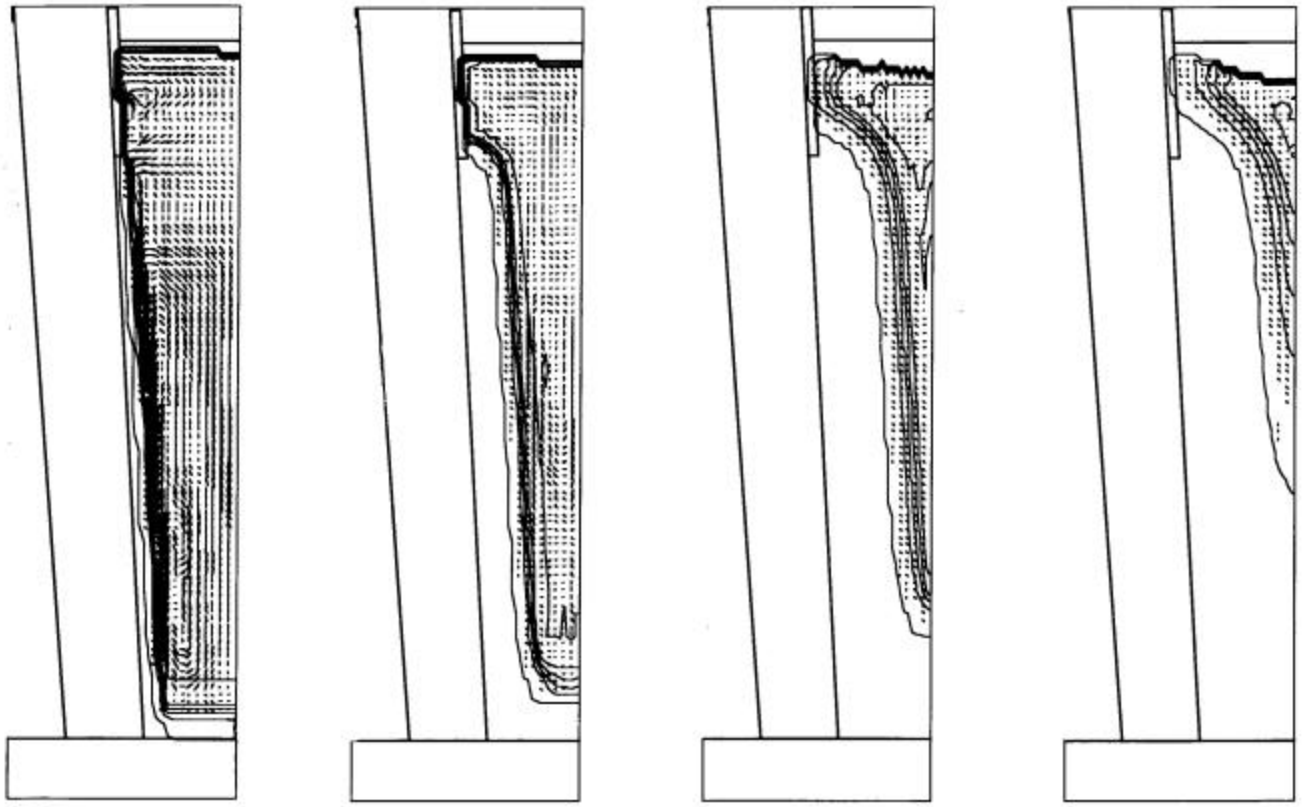

*(a)* 500 s *(b)* 3000 s *(c)* 9000 s *(d)* 15000 s

Figure 4: Predicted velocity vectors (the largest arrow corresponds to approximately 2.5 cm/s) and solid fraction contours (in 20 pct increments) at various times during solidification of a steel ingot [27].

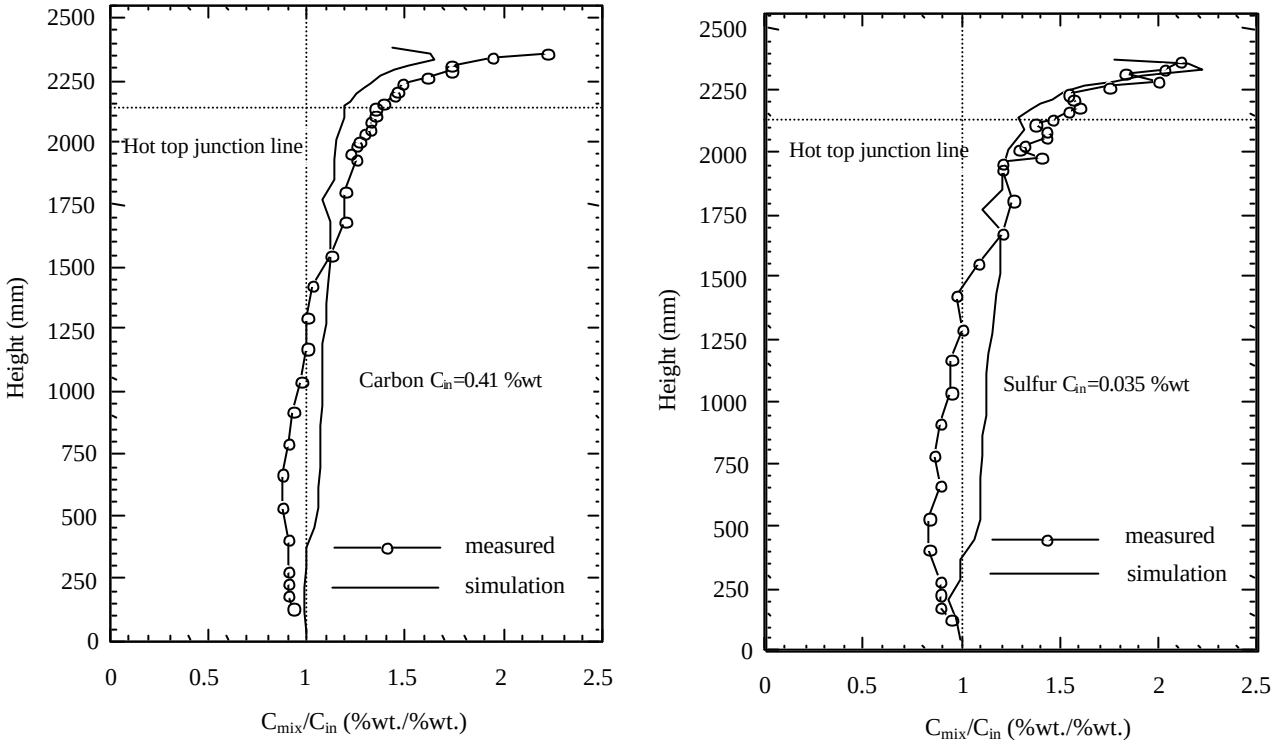


*(a)* carbon *(b)* sulfur

Figure 5: Comparison of measured and predicted macrosegregation variations along the vertical centerline of a steel ingot [27].

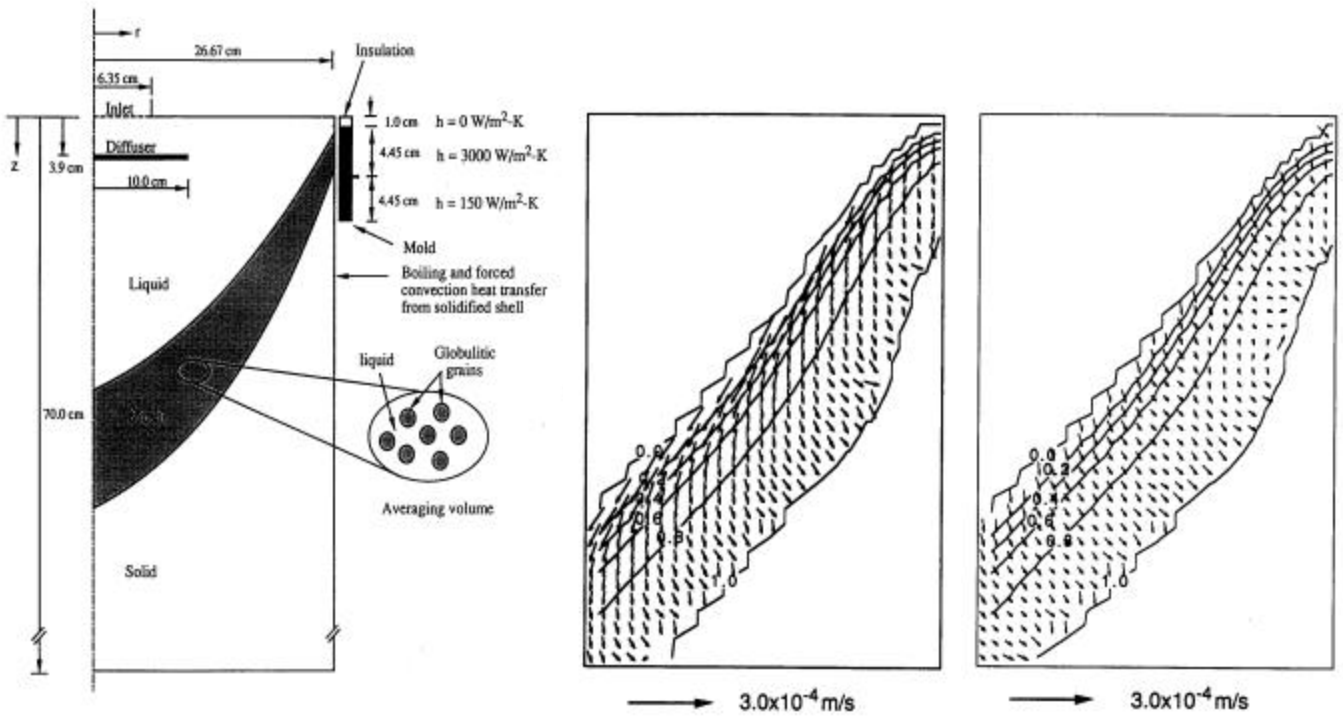


*(a)* simulation domain *(b)* with grain refiner *(c)* without grain refiner

Figure 6: Simulation of macrosegregation in DC casting of an Al-4.5 wt% Cu cylindrical ingot; *(a)* schematic illustration of the simulation domain; *(b)* and *(c)* predicted relative velocities and solid fraction contours inside the mushy zone near the mold for simulations with and without grain refiner, respectively [30].

segregation due to shrinkage-driven flow and exudation was observed at the ingot surface. Results from numerical simulations of these experiments are shown in Figure 6 and Figure 7 [30]. Close-ups of predicted relative liquid velocities and solid fraction contours inside the mushy zone near the mold are shown in Figs. 6b and 6c for the grain-refined and non-grain-refined cases, respectively. In both cases, it can be seen that there exists a shrinkage-driven flow towards the eutectic front. In the grain-refined case (Fig. 6b), with a more permeable mushy zone, a relatively strong thermosolutal buoyancy-driven flow towards the ingot centerline is present in the lower solid fraction region of the mush. As measured in the experiments, the simulations showed that the buoyancy-driven flow in the grain-refined case (Fig. 7a) produces positive centerline macrosegregation. On the other hand, in the non-grain-refined case (Fig. 7b), the shrinkage-driven flow, together with the weakness of buoyancy-driven flow, results in negative centerline macrosegregation. Due to the neglect of exudation, the extent of positive inverse segregation at the ingot surface is somewhat underpredicted. The above comparison shows that the macrosegregation model predicts the correct macrosegregation trends and magnitudes, and it illustrates the strong effect of the microstructure. However, the grain sizes and dendrite arm spacings needed in the permeability model were taken from the experiments. A truly predictive model would also need to predict the microstructure. Furthermore, it has been argued that the transport of broken/detached solid fragments and equiaxed grains from the mold region to the ingot center tends to cause negative centerline macrosegregation in commercial Al ingots. Preliminary simulations with a two-phase model support this conclusion [31]. Nonetheless, the simulation of the transport during solidification of the complex multicomponent alloys used in actual DC-casting processes, concurrently with the prediction of grain structure development, is still lacking.

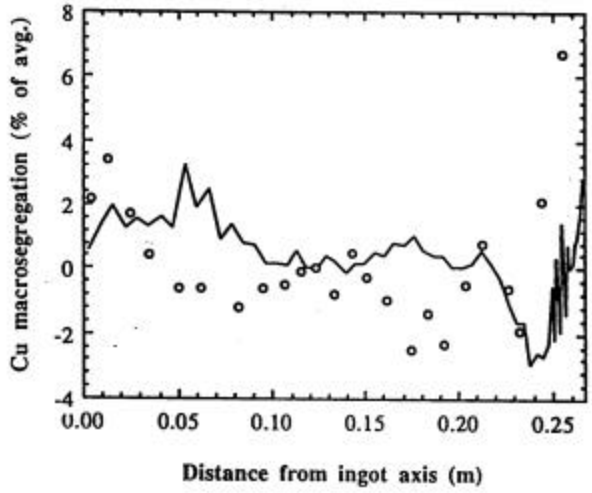


*(a)* with grain refiner

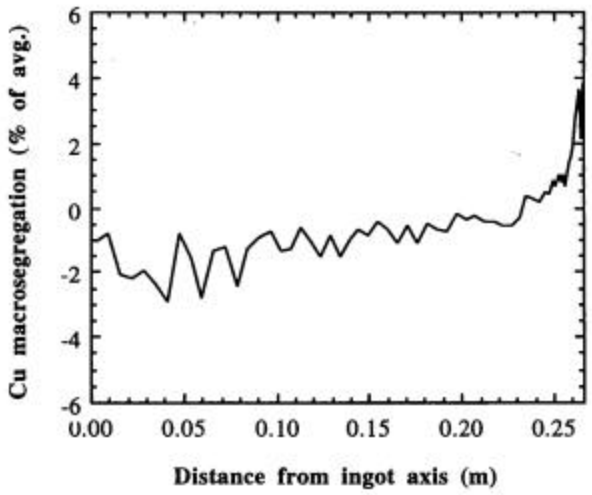


*(b)* without grain refiner

Figure 7: Simulation of macrosegregation in DC casting of an Al-4.5 wt% Cu cylindrical ingot; *(a)* comparison of measured (symbols) and predicted (line) radial macrosegregation profiles in the grain-refined experiment of Finn et al. [29], *(b)* predicted radial macrosegregation profile in a simulation without grain refiner [30].

*Example 3: Single-Crystal Ni-base Superalloy Casting*

The third example is concerned with the simulation of freckling in upward directional solidification of single-crystal Ni-base superalloys. Figure 8 shows photos of such freckles in an experimental superalloy casting. Typical predictions from a two-dimensional micro-/macrosegregation model [32] are presented in Fig. 9. The novel feature of this model is that phase equilibrium was calculated at each time step using a previously developed thermodynamic subroutine for multicomponent Ni-base superalloys. The open channels in the mush through which enriched liquid streams upward into the bulk melt are predicted realistically. These channels later fill with equiaxed grains and become freckles. Although three-dimensional calculations have been reported recently by Felicelli et al. [33], extension of such simulations to actual cast components is difficult, due to the large computer resources required to resolve such small macrosegregation features over the scale of the entire component. For this reason, a simpler freckle predictor was developed that relies on the calculation of a local mush Rayleigh number [34]. Figure 10 shows the variation of the Rayleigh number with the local thermal conditions (temperature gradient, $\boldsymbol{G}$, and isotherm speed, $R$). The symbols in Fig. 10 correspond to the experiments of Pollock and Murphy [35]. Based on their measurements of freckle occurrence, a critical Rayleigh number for freckle

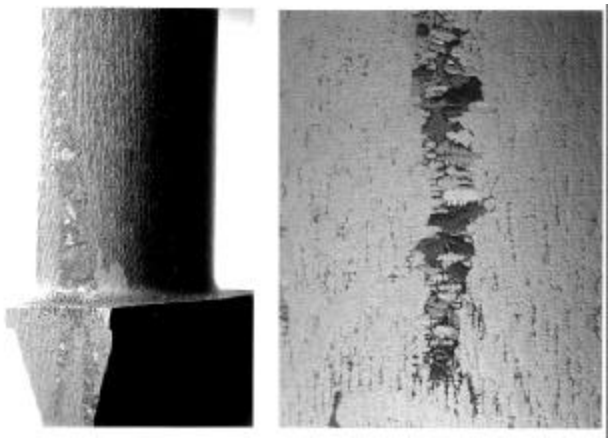

Figure 8: Freckles in a single-crystal Ni-base superalloy prototype blade (left panel) and close-up of a single freckle (right panel) (courtesy of A.F. Giamei, United Technologies Research Center).

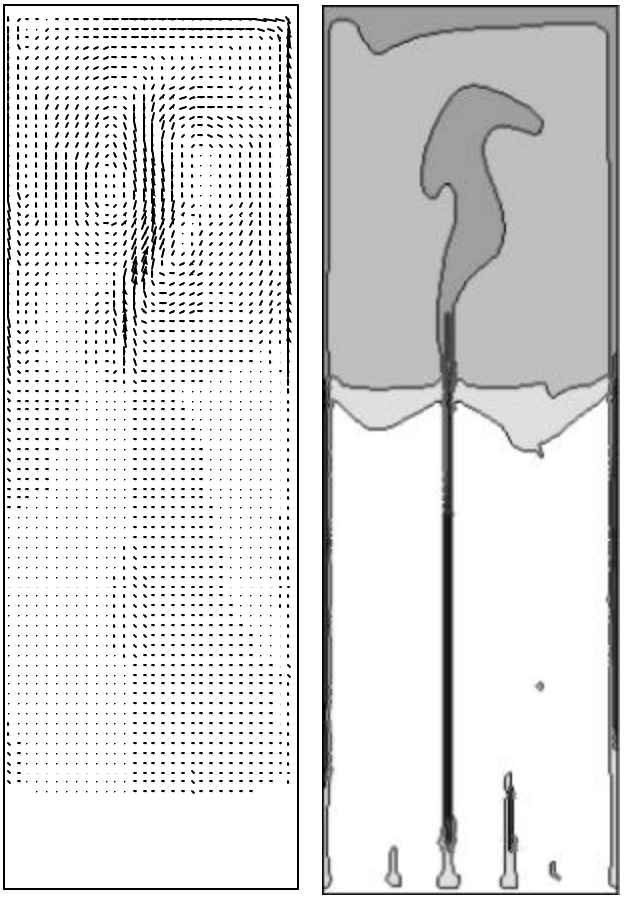

Figure 9: Predicted velocity vectors and solid fraction contours (left panel) and macrosegregation pattern (right panel) showing freckle formation during directional solidification of a single-crystal Ni-base superalloy [32].

formation can be identified. The critical Rayleigh number derived from experiments agrees with the value corresponding to freckle initiation in simulations [34]. Figure 11 shows how additional simulations can then be used, instead of experiments, to determine the variation of the critical Rayleigh number with the inclination of the domain with respect to gravity.

*Example 4: Complex Steel Casting*

The final example illustrates that macrosegregation due to interdendritic flow can now be simulated for the complex, three-dimensional castings commonly encountered in foundry practice. Figure 12 shows examples from a user-friendly casting simulation software package of macrosegregation calculations for a large production steel casting [36]. The left panel is a plot of the predicted convection patterns in the bulk liquid and mushy zones during solidification. The right panel shows the predicted carbon macrosegregation pattern in the fully solidified casting, indicating an under-riser segregation problem. Extensive efforts at several foundries are underway to apply this software and compare the macrosegregation predictions to measurements from production castings. As in the previous examples, the resolution of small-scale macrosegregation features, such as A-segregates or freckles, in large castings is beyond the current capabilities of this software.

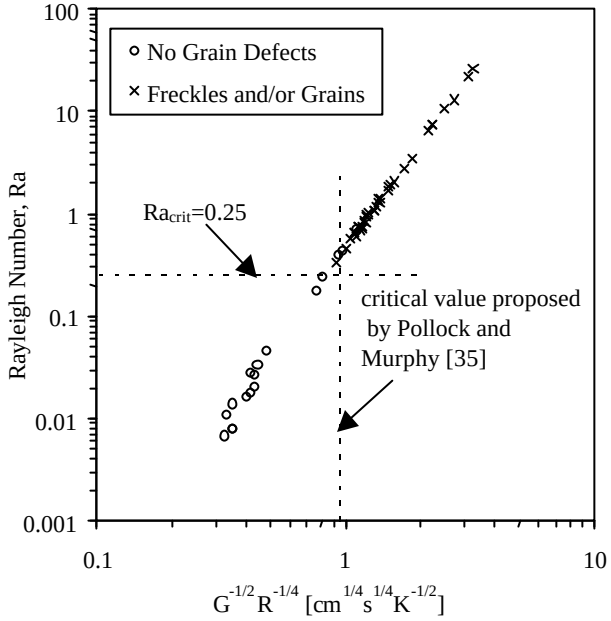


Figure 10: Variation of the mush Rayleigh number with the local thermal conditions in the experiments of Pollock and Murphy [35] on directional solidification of single-crystal Ni-base superalloys; no freckles form below the critical mush Rayleigh number of 0.25 [34].

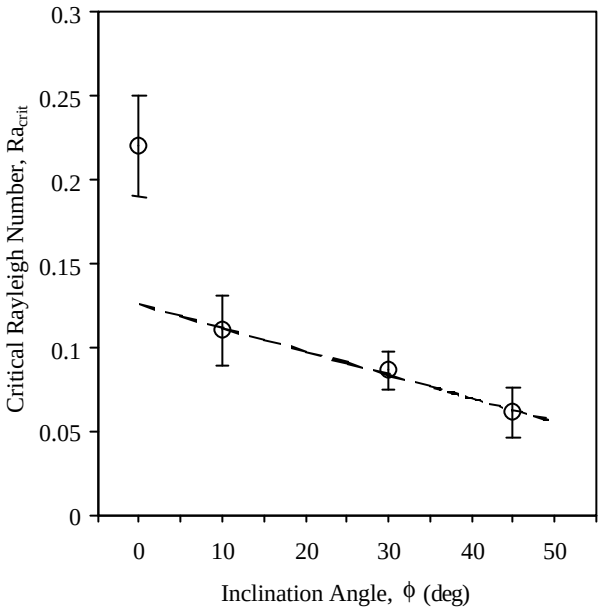


Figure 11: Simulation results for the dependence of the critical mush Rayleigh number for freckle initiation in directional solidification of single-crystal Ni-base superalloys on the inclination of the domain with respect to gravity [34].

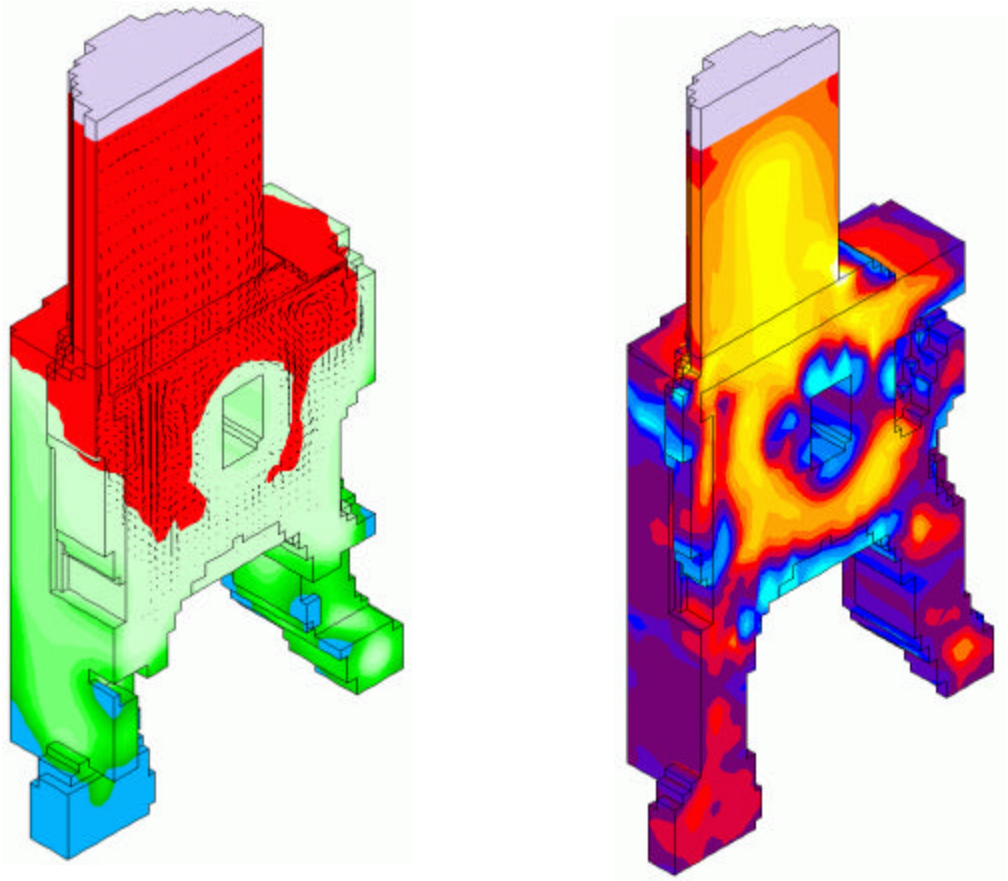

Figure 12: Simulation of macrosegregation formation in a complex steel casting (left panel: liquid velocity vectors during solidification; right panel: final carbon macrosegregation pattern) [36].

Coupled Microstructure-Macrosegregation Models

The examples of the previous sections illustrate that the microstructure of castings has a profound influence on macrosegregation. Many macrosegregation features cannot be predicted without detailed consideration of the microstructure. Further progress in macrosegregation modeling can only be made if the microstructure is predicted as well. This section highlights recent efforts to develop coupled microstructure-macrosegregation models. A more thorough review of past work in this area is available [1].

The most obvious example of this interdependency is the variation of permeability with microstructure. In directional solidification (i.e., columnar dendritic growth), the dendrite arm spacings are the primary microstructural parameters that affect the permeability, and much work has been performed to measure the permeability for such systems (see for example Ref. [37]). However, most castings (both continuous and static) feature zones of equiaxed grains or are fully equiaxed. In the equiaxed case, both the grain density and the structure of individual grains influence the permeability, as shown theoretically by Wang et al. [38] and verified experimentally for aluminum alloys by Nielsen et al. [39]. The situation is further complicated by the fact that small dendrite fragments or equiaxed grains can move in the melt before forming a coherent solid, resulting in macrosegregation by settling (or flotation). The drag coefficients of single equiaxed grains have also been measured and correlated recently [40].

The microstructure affects macrosegregation not only through the permeability of a coherent mush or the drag coefficient of free grains. Different microstructures also result in different flow patterns, latent heat evolutions, and microscopic solute rejection (microsegregation) behaviors, all of which influence macrosegregation. Furthermore, the melt must undercool before nucleation and growth can proceed; however, all of the previously reviewed macrosegregation models assume that the liquid is in equilibrium and locally well mixed (as in the Scheil or Lever rule models). In reality, all castings with equiaxed structures feature undercooled liquid regions during solidification where the equiaxed grains grew. For example, M'Hamdi et al. [41] recently estimated that in continuous casting of steel, there is an undercooled liquid zone several meters in height. A large undercooled zone has also been predicted for DC-casting of aluminum [31]. Even in purely columnar growth, there is a potentially large undercooled liquid region in front of the primary dendrite tips, especially when the thermal gradient is low (such as in sudden cross-section expansions in casting of single-crystal turbine blades). Although the level of undercooling may be no more than a few degrees in traditional casting processes, its consideration is crucial when modeling coupled microstructure-macrosegregation development.

Much of the progress prior to 1989 in modeling microstructure formation in castings has been summarized by Rappaz [42]. More recent efforts, including approximate treatments of convection, have been reviewed by Gandin et al. [43]. However, the only

models to date that consider macrosegregation (as well as growth into an undercooled melt, melt convection, and grain movement) are the two-phase model of Ni and Beckermann [44] and the multi-phase/-scale model of Wang and Beckermann [1, 45-51]. In the derivation of the latter models, the microscopic (or point) conservation equations for each phase are formally averaged over a representative elementary volume (REV), like the one shown in Fig. 2. The averaging results in separate macroscopic conservation equations for each phase and averaged interface conditions that can be solved using a single-domain approach for the entire casting. The key advantages of a formal averaging procedure are:

- The macroscopic variables, such as the average solute concentration in the solid in the REV, are defined in terms of the microscopic profiles.
- Each term in the averaged equations has a clear origin, and terms accounting for the latent heat, permeability, nucleation rate, dendrite tip growth, etc. *naturally* arise from the averaging procedure; this point may seem unimportant, but there has, in fact, been considerable controversy over the correct form of some of the equations [22, 23, 52] and some confusion over how to best incorporate, for example, columnar dendrite tip undercooling in macroscopic models [53, 54].
- Most importantly, the averaged conservation equations explicitly contain micro-scale parameters such as the phase volume fractions, grain density, interfacial area concentration, local diffusion lengths, drag coefficients, etc.

References [46-48] contain a number of applications of the multi-phase/-scale model to various solidification systems where flow can be neglected.

The application of the multi-phase/-scale model to solidification with simultaneous melt convection and grain movement is illustrated in the following example [50]. An Al-4 wt% Cu alloy solidifies in an equiaxed dendritic fashion inside a rectangular cavity cooled from the left sidewall. Figure 13 shows the predicted evolution of the grain density (i.e., number of grains per unit volume). Free grains nucleate first near the cooled sidewall and are swept into the central part of the cavity by the thermosolutal melt convection. The small nuclei grow in those regions of the cavity where the melt is undercooled and remelt where the melt is still superheated. Later, when the grains have grown to a sufficient size, they settle and form a fixed bed of equiaxed crystals at the bottom of the cavity. This bed continues to grow in height as more free grains settle downward. The interface between the bed and the overlying region of undercooled melt, containing freely moving and growing grains, is characterized by a relatively sharp gradient in the grain density. The grain density in the bed itself is invariant, and the melt inside the bed is not undercooled. Upon complete solidification, a reduced grain density and, hence, larger grains, can be observed in the upper part of the cavity, which can be attributed to the continuous sedimentation of grains out of this region. Because the local nucleation rate was set to a constant value, the grain density would have been uniform in the absence of grain movement. Therefore, all spatial variations in the grain density are directly related to grain movement.

The effects of grain movement, and different nucleation rates, on macrosegregation are illustrated in Fig. 14. Figure 14a corresponds to a simulation where a stationary solid phase was assumed. Thermosolutal convection causes strong positive

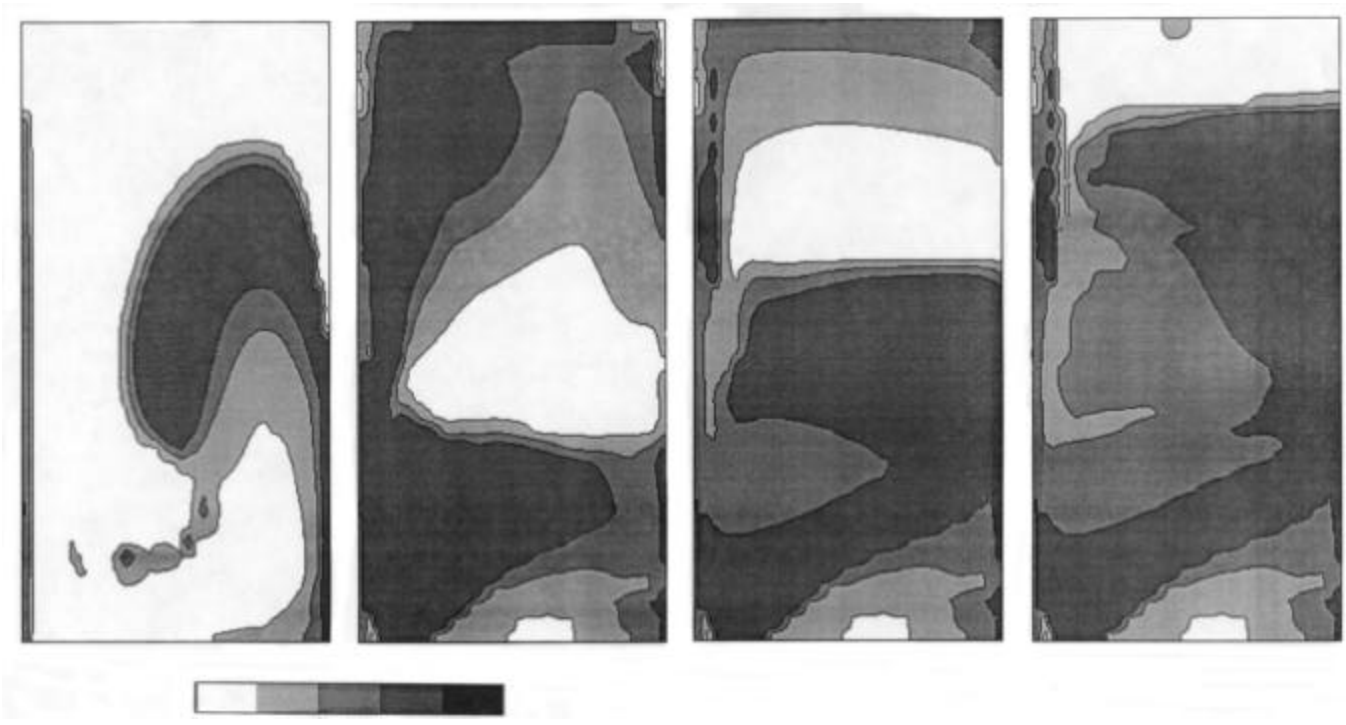


Figure 13: Predicted evolution of the grain density during equiaxed dendritic solidification of an Al-4 wt% Cu alloy with grain movement inside a rectangular cavity cooled from the left sidewall [50].

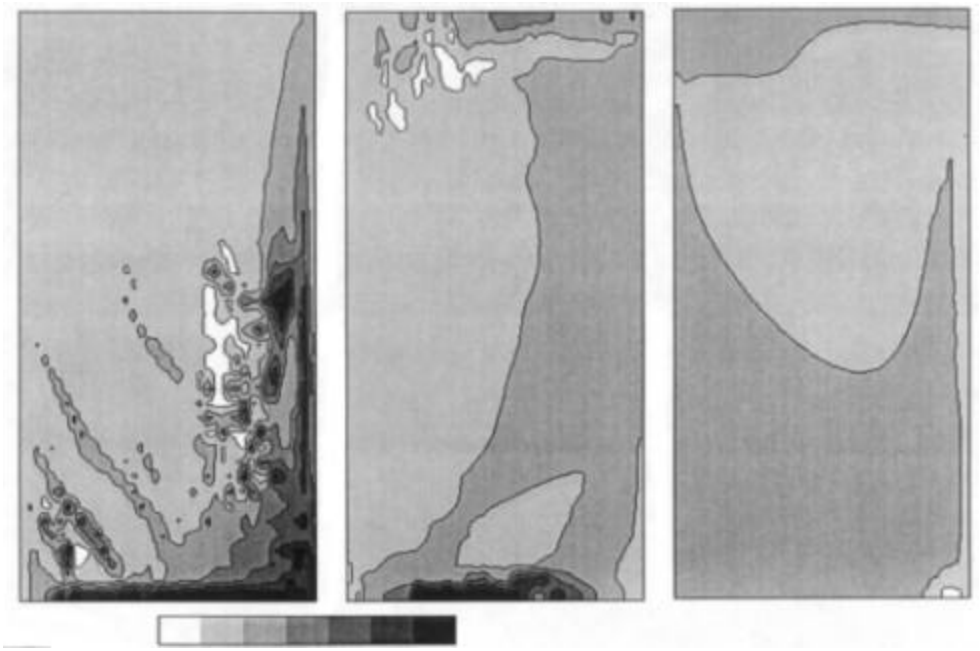


*(a)* stationary grains (low nucleation rate) | *(b)* moving grains (low nucleation rate) | *(c)* moving grains (high nucleation rate)

Figure 14: Effect of grain movement, and different nucleation rates, on predicted macrosegregation patterns in equiaxed dendritic solidification of an Al-4 wt% Cu alloy inside a rectangular cavity cooled from the left sidewall [50].

macrosegregation along the bottom wall and right sidewall of the cavity because the solute-rich, cold melt is heavy and flows downward during solidification. In addition several (inverted) A-segregates can be observed in the lower central region. Figure 14b shows the macrosegregation pattern for a simulation with moving grains, corresponding to the grain density plots of Fig. 13. Overall, the macrosegregation is less severe and no channel segregates are predicted. This can be attributed to the fact that both the solute-rich liquid and the solute-poor solid flow together downward, resulting in less relative motion between the solid and liquid phases than in the case of a stationary solid. Even less macrosegregation is observed in Fig. 14c, where a higher nucleation rate was employed in the simulation. The higher nucleation rate results in smaller grains that closely follow the liquid motion until they pack. It should be noted that in alloys where the solute-rich liquid is lighter and the solid is more dense than the melt of the original composition, the settling of free grains causes negative macrosegregation at the bottom and positive macrosegregation at the top of the solidification domain. The classical macrosegregation pattern in a steel ingot (Fig. 3) may be an example of that effect. However, in the Al-Cu system of Figs. 13 and 14, the solute-rich melt is heavier and the positive macrosegregation at the bottom of the cavity due to melt flow (Fig. 14a) is partially "canceled" by the settling of solute-poor solid, resulting in less severe overall macrosegregation (Figs. 14b and c).

A comparison of the multi-phase/-scale model with experiments conducted using the transparent model alloy $NH_4Cl$-$H_2O$ revealed good agreement between the measured and predicted flow patterns and crystal settling rates during solidification [51]. While the multi-phase/-scale model appears to provide a suitable framework for coupled microstructure-macrosegregation modeling, many uncertainties still exist. For example, only approximate models are available for the effect of flow on grain generation (including fragmentation), dendrite tip growth, two-phase rheology, etc. Concentrated research efforts are underway to clarify these and other questions (see for example [55-57]), but much work remains.

## Related Developments

During the last decade, much progress has been made in the direct numerical simulation of solidification microstructure development. In particular, the phase-field method has been used to predict a variety of complex growth patterns from first principles [58-60]. Beckermann et al. [61] have extended the phase-field method to include melt convection. This new capability will allow for the detailed investigation of the effects of flow on the structure of the mush, dendrite tip growth [62], microsegregation, fragmentation, and other flow related issues that have hampered coupled microstructure-macrosegregation modeling in the past. This modeling work is of particular importance since such investigations are difficult to perform experimentally owing to the small scale of the phenomena involved.

An example of a microstructure simulation that has a direct bearing on modeling of macrosegregation is the recent study of Diepers et al. [63]. They used the phase-field method to model the flow through, and ripening of, an adiabatic Al-4 wt% Cu alloy mush volume element, like the one shown in Fig. 2. Representative two-dimensional simulation results with and without flow are shown in Fig. 15. Ripening (or coarsening)

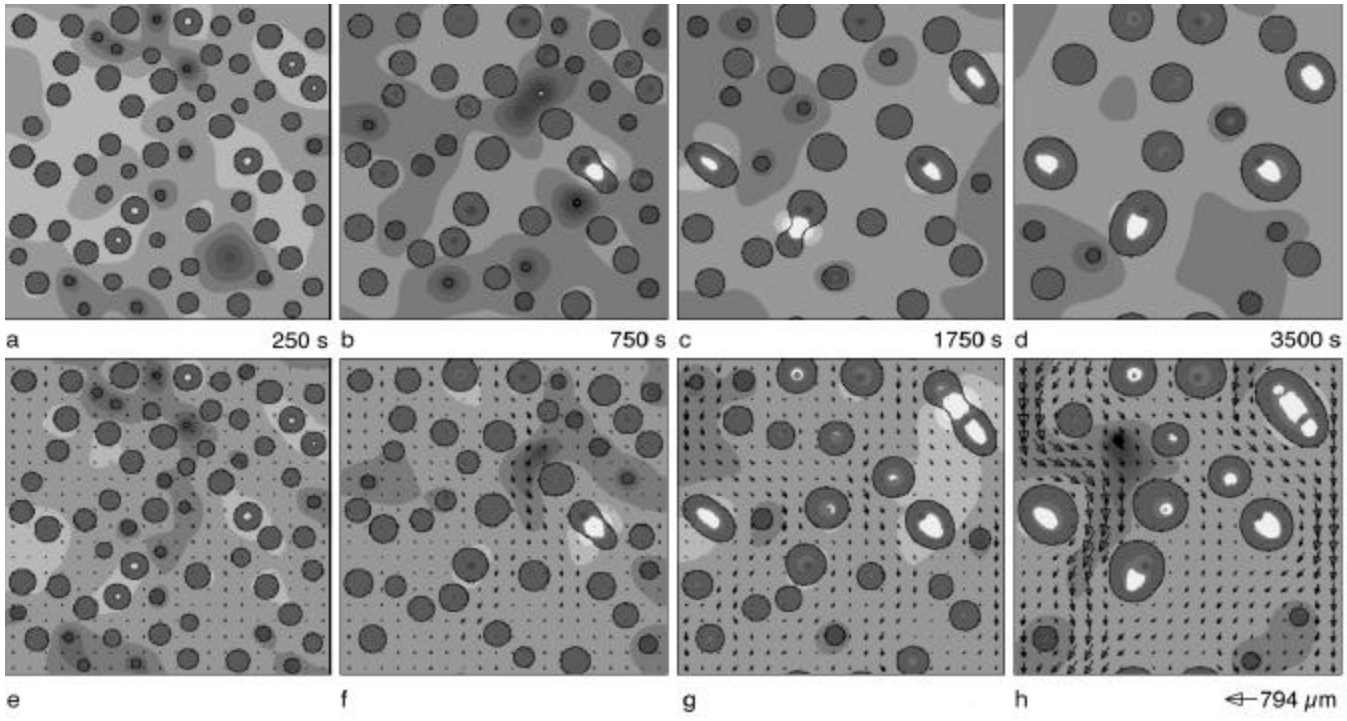


Figure 15: Phase-field simulations of the evolution of the microstructure due to Ostwald ripening in an Al-4 wt% Cu alloy mush where the solid fraction is constant at 20%; the black contour lines show the solid-liquid interface and the gray shades indicate the Cu concentrations in the liquid and solid: *(a)* to *(d)* are for a simulation under purely diffusive conditions; *(e)* to *(h)* are for a simulation with forced convection in the north-south direction (arrows are liquid velocity vectors) [63].

causes the solid/liquid interfacial area to decrease with time. This, in turn, results in an increase in the permeability. However, it is important to realize that the ripening dynamics are influenced by convection. In other words, the microstructure of the mush not only governs the flow, but the flow also influences the evolution of the microstructure. The simulations of Diepers et al. verified that, in accordance with classical ripening theories, the interfacial area decreases with the cube root of time in the case of no flow. In the presence of flow, on the other hand, the interfacial area decreases with the square root of time. Diepers et al. also calculated the permeability of the mush volume element and found that the permeability normalized by the square of the interfacial area per unit solid volume is constant in time. By performing simulations with different volume fractions of solid inside the element, they were able to correlate the permeability with the various microstructural parameters present.

While knowledge of the permeability of an evolving microstructure is important for present macrosegregation models, the simulations of Diepers et al. [63] also point the way toward the future of macrosegregation modeling through numerical simulations on the microscopic scale. In this way, all of the microscopic phenomena would be directly taken into account, and the results could be used to assess and improve models that are based on averaging, such as the ones reviewed in the previous two sections. Presently, such microscopic simulations of macrosegregation formation cannot be performed on the scale of an entire casting. However, with some evolution in computing power, they would be realistic for scales of the order of several millimeters (requiring of the order of $10^9$ to $10^{12}$ grid points in three dimensions).

## Conclusions and Future Research Needs

The pioneering work of Flemings and coworkers in the mid-1960s has led to major advances in understanding and predicting the complex transport and macrosegregation phenomena in solidification of alloy castings. Since then, models have been developed to predict macrosegregation patterns in a variety of industrially relevant casting processes. While some successes have been reported in predicting measured macrosegregation patterns, there are still numerous areas where further development is required. The following basic phenomena should receive increased research attention:

- macrosegregation in multicomponent alloys, taking into account the formation of multiple phases and grain structure transitions (e.g., columnar-to-equiaxed);
- macrosegregation due to deformation of the solid or mush;
- macrosegregation due to movement of solid;
- macrosegregation formation in the presence of undercooled, convecting liquid.

Furthermore, the resolution of melt flow patterns in numerical solutions of macrosegregation models often has been inadequate, and most simulations reported in the literature are restricted to two dimensions. With the availability of increased computing power and more efficient numerical techniques, greater attempts should be made to reduce numerical inaccuracies and to resolve the highly three-dimensional and transient (or oscillatory) flow patterns present in solidification systems.

It has become clear that numerous macrosegregation phenomena cannot be predicted without detailed consideration of the evolving microstructure. Thus, in many cases, further progress in macrosegregation modeling can only be made if the

microstructure and grain structure transitions are predicted as well. While research in the area of solidification microstructures has traditionally focused on the prediction of phases and growth patterns in a diffusive environment, macrosegregation modeling requires a quantitative understanding of the convective interactions on a microscopic scale. A few of the outstanding research issues are:

- nucleation in a convective environment;
- fragmentation and transport of fragments originating in the mushy zone or at outer surfaces;
- effects of flow on the growth rates of the dendrite tips, eutectic front, etc.;
- effects of flow on the evolution of dendrite arm spacings and other microstructural length scales; and
- two-phase rheology of a melt laden with equiaxed grains.

Future research on any of the above issues will increasingly rely on first-principles, direct numerical simulations of solidification with flow on a microscopic scale using, for example, the phase-field method. These advances in modeling are especially important in light of the difficulties in performing accurate experimental measurements on a microscopic scale. However, the use of such micro-scale simulations to predict macrosegregation on the scale of an entire casting will not be an option until at least my 70$^{th}$ birthday.

## Acknowledgements

The author would like to thank his present and former graduate students and other researchers who have contributed to some of the work reviewed in this article. The writing of this article was made possible, in part, through the support of NASA under Contract No. NCC8-94.

## References

1. C. Beckermann and C.Y. Wang, "Multi-Phase/-Scale Modeling of Transport Phenomena in Alloy Solidification," in Annual Review of Heat Transfer VI, vol. 6, ed. C.L. Tien (New York, NY: Begell House, 1995), 115-198.

2. P.J. Prescott and F.P. Incropera, "Convection Heat and Mass Transfer in Alloy Solidification," in Advances in Heat Transfer, ed. D. Poulikakos (San Diego, CA: Academic Press, 1996), 231-338.

3. H. Combeau, B. Appolaire and G. Lesoult, "Recent Progress in Understanding and Prediction of Macro and Mesosegregations," in Modeling of Casting, Welding and Advanced Solidification Processes – VIII, ed. B.G. Thomas and C. Beckermann (Warrendale, PA: TMS, 1998), 245-256.

4. M.C. Flemings, "Solidification Modeling, Past and Present," in Modeling of Casting, Welding and Advanced Solidification Processes – VIII, ed. B.G. Thomas and C. Beckermann (Warrendale, PA: TMS, 1998), 1-13.

5. M.C. Flemings and G.E. Nereo, "Macrosegregation: Part I," Trans. AIME, 239 (1967), 1449-1461.

6. M.C. Flemings, R. Mehrabian and G.E. Nereo, "Macrosegregation: Part II," Trans. AIME, 242 (1968), 41-49.

7. M.C. Flemings and G.E. Nereo, "Macrosegregation: Part III," Trans. AIME, 242 (1968), 50-55.

8. R. Mehrabian, M. Keane and M.C. Flemings, "Interdendritic Fluid Flow and Macrosegregation; Influence of Gravity," Metall. Trans., 1 (1970), 1209-1220.

9. T.S. Piwonka and M.C. Flemings, "Pore Formation in Solidification," Trans. AIME, 236 (1966), 1157-1165.

10. D. Apelian, M.C. Flemings and R. Mehrabian, "Specific Permeability of Partially Solidified Dendritic Networks of Al-Si Alloys," Metall. Trans., 5 (1974), 2533-2537.

11. R. Mehrabian, M.A. Keane and M.C. Flemings, "Experiments on Macrosegregation and Freckle Formation," Metall. Trans., 1 (1970), 3238-3241.

12. S. Kou, D.R. Poirier and M.C. Flemings, "Macrosegregation in Rotated Remelted Ingots," Metall. Trans. B, 9 (1978), 711-719.

13. R. Mehrabian and M.C. Flemings, "Macrosegregation in Ternary Alloys," Metall. Trans., 1 (1970), 455-464.

14. T. Fujii, D.R. Poirier and M.C. Flemings, "Macrosegregation in a Multicomponent Low Alloy Steel," Metall. Trans. B, 10 (1979), 331-339.

15. S.D. Ridder, S. Kou and R. Mehrabian, "Effect of Fluid Flow on Macrosegregation in Axi-Symmetric Ingots," Metall. Trans. B, 12 (1981), 435-447.

16. V.C. Prantil and P.R. Dawson, "Application of Mixture Theory to Continuous Casting," in HTD-Vol. 29 (New York, NY: ASME, 1983), 47-54.

17. R.N. Hills, D.E. Loper and P.H. Roberts, "A Thermodynamically Consistent Model of a Mushy Zone," Q. J. Mech. Appl. Math., 36 (1983), 505-539.

18. D.A. Drew, "Mathematical Modeling of Two-Phase Flow," Ann. Rev. Fluid Mech., 15 (1983), 261-291.

19. W.D. Bennon and F.P. Incropera, "A Continuum Model for Momentum, Heat and Species Transport in Binary Solid-Liquid Phase Change Systems. I. Model Formulation," Int. J. Heat Mass Transfer, 30 (1987), 2161-2170.

20. C. Beckermann and R. Viskanta, "Double-Diffusive Convection during Dendritic Solidification of a Binary Mixture," PhysicoChemical Hydrodynamics, 10 (1988), 195-213.

21. V.R. Voller, A.D. Brent and C. Prakash, "The Modelling of Heat, Mass and Solute Transport in Solidification Systems," Int. J. Heat Mass Transfer, 32 (1989), 1718-1731.

22. S. Ganesan and D.R. Poirier, "Conservation of Mass and Momentum for the Flow of Interdendritic Liquid during Solidification," Metall. Trans. B, 21 (1990), 173-181.

23. D.R. Poirier, P.J. Nandapurkar and S. Ganesan, "The Energy and Solute Conservation Equations for Dendritic Solidification," Metall. Trans. B, 22 (1991), 889-900.

24. W.D. Bennon and F.P. Incropera, "The Evolution of Macrosegregation in Statically Cast Binary Ingots," Metall. Trans. B, 18 (1987), 611-616.

25. M.G. Worster, "Convection in Mushy Layers," Ann. Rev. Fluid Mech., 29 (1997), 91-122.

26. M.C. Flemings, Solidification Processing, (New York, NY: McGraw Hill, 1974).

27. J.P. Gu and C. Beckermann, "Simulation of Convection and Macrosegregation in a Large Steel Ingot," Metall. Mater. Trans. A, 30 (1999), 1357-1366.

28. M.C. Schneider and C. Beckermann, "Formation of Macrosegregation by Multicomponent Thermosolutal Convection during Solidification of Steel," Metall. Mater. Trans. A, 26 (1995), 2373-2388.

29. T.L. Finn, M.G. Chu and W.D. Bennon, "The Influence of Mushy Region Microstructure on Macrosegregation in Direct Chill Cast Aluminum-Copper Round Ingots," in Micro/Macro Scale Phenomena in Solidification, ed. C. Beckermann et al. (New York, NY: ASME, 1992), 17-26.

30. A.V. Reddy and C. Beckermann, "Modeling of Macrosegregation due to Thermosolutal Convection and Contraction-Driven Flow in Direct Chill Continuous Casting of an Al-Cu Round Ingot," Metall. Mater. Trans. B, 28 (1997), 479-489.

31. A.V. Reddy and C. Beckermann, "Simulation of the Effects of Thermosolutal Convection, Shrinkage Induced Flow and Solid Transport on Macrosegregation and Equiaxed Grain Size Distribution in a DC Continuous Cast Al-Cu Round Ingot," in Materials Processing in the Computer Age - II, ed. V.R. Voller et al. (Warrendale, PA: TMS, 1995), 89-102.

32. M.C. Schneider et al., "Modeling of Micro- and Macrosegregation and Freckle Formation in Single-Crystal Nickel-Base Superalloy Directional Solidification," Metall. Mater. Trans. A, 28 (1997), 1517-1531.

33. S.D. Felicelli, D.R. Poirier and J.C. Heinrich, "Modeling of Freckle Formation in Three Dimensions during Solidification of Multicomponent Alloys," Metall. Mater. Trans. B, 29 (1998), 847-855.

34. C. Beckermann, J.P. Gu and W.J. Boettinger, "Development of a Freckle Predictor for Single-Crystal Nickel-Base Superalloy Castings," Metall. Mater. Trans. A, (2000), in press.

35. T.M. Pollock and W.H. Murphy, "The Breakdown of Single-Crystal Solidification in High Refractory Nickel-Base Alloys," Metall. Mater. Trans. A, 27 (1996) 1081-1094.

36. M.C. Schneider et al., "Macrosegregation Formation During Solidification of Complex Steel Castings: 3-D Numerical Simulation and Experimental Comparison," in Modeling of Casting, Welding and Advanced Solidification Processes - VIII, ed. B.G. Thomas and C. Beckermann (Warrendale, PA: TMS, 1998), 257-264.

37. D.R. Poirier, "Permeability for Flow of Interdendritic Liquid in Columnar-Dendritic Alloys," Metall. Trans. B, 18 (1987), 245-255.

38. C.Y. Wang et al., "Multiparticle Interfacial Drag in Equiaxed Solidification," Metall. Trans. B, 26 (1995), 111-119.

39. O. Nielsen et al., "Experimental Determination of Mushy Zone Permeability in Aluminum-Copper Alloys with Equiaxed Microstructures," Metall. Mater. Trans. A, 30 (1999), 2455-2462.

40. H.C. de Groh III et al., "Calculation of Dendrite Settling Velocities Using a Porous Envelope," Metall. Trans. B, 24 (1993), 749-753.

41. M. M'Hamdi et al., "Numerical Modeling of the Columnar to Equiaxed Transition in Continuous Casting of Steel," in Modeling of Casting, Welding and Advanced Solidification Processes - VIII, ed. B.G. Thomas and C. Beckermann (Warrendale, PA: TMS, 1998), 375-382.

42. M. Rappaz, "Modeling of Microstructure Formation in Solidification Processes," Int. Mater. Rev., 34 (1989), 93-123.

43. Ch.-A. Gandin, T. Jalanti and M. Rappaz, "Modeling of Dendritic Grain Structures," in Modeling of Casting, Welding and Advanced Solidification Processes - VIII, ed. B.G. Thomas and C. Beckermann (Warrendale, PA: TMS, 1998), 363-374.

44. J. Ni and C. Beckermann, "A Volume-Averaged Two-Phase Model for Solidification Transport Phenomena," Metall. Trans. B, 22 (1991), 349-361.

45. C.Y. Wang and C. Beckermann, "Single- vs. Dual-Scale Volume Averaging for Heterogeneous Multiphase Systems," Int. J. Multiphase Flow, 19 (1993), 397-407.

46. C.Y. Wang and C. Beckermann, "A Multiphase Solute Diffusion Model for Dendritic Alloy Solidification," Metall. Trans. A, 24 (1993), 2787-2802.

47. C.Y. Wang and C. Beckermann, "A Unified Solute Diffusion Model for Columnar and Equiaxed Dendritic Alloy Solidification," Mater. Sci. Eng. A, 171 (1993), 199-211.

48. C.Y. Wang and C. Beckermann, "Prediction of Columnar to Equiaxed Transition During Diffusion-Controlled Dendritic Alloy Solidification," Metall. Trans. A, 25 (1994), 1081-1093.

49. C.Y. Wang and C. Beckermann, "Equiaxed Dendritic Solidification with Convection: Part 1. Multi-Scale /-Phase Modeling," Metall. Mater. Trans. A, 27 (1996), 2754-2764.

50. C.Y. Wang and C. Beckermann, "Equiaxed Dendritic Solidification with Convection: Part 2. Numerical Simulations for an Al-4 wt% Cu Alloy," Metall. Mater. Trans. A, 27 (1996), 2765-2783.

51. C. Beckermann and C.Y. Wang, "Equiaxed Dendritic Solidification with Convection: Part 3. Comparisons with $NH_4Cl$-$H_2O$ Experiments," Metall. Mater. Trans. A, 27 (1996), 2784-2795.

52. P.J. Prescott, F.P. Incropera and W.D. Bennon, "Modeling of Dendritic Solidification Systems: Reassessment of the Continuum Momentum Equation," Int. J. Heat Mass Transfer, 34 (1991), 2351-2359.

53. I. Dustin and W. Kurz, "Modeling of Cooling Curves and Microstructures During Equiaxed Dendritic Solidification," Z. Metallkd., 77 (1986), 265-273.

54. S.C. Flood and J.D. Hunt, "A Model of a Casting," Appl. Sci. Res., 44 (1987), 27-42.

55. C.J. Paradies et al., "The Effect of Flow Interactions with Dendritic Mushy Zones: A Model Experiment," in Modeling of Casting, Welding and Advanced Solidification Processes - VI, ed. T.S. Piwonka et al. (Warrendale, PA: TMS, 1993), 309-316.

56. A. Ramani and C. Beckermann, "Dendrite Tip Growth Velocities of Settling $NH_4Cl$ Equiaxed Crystals," Scripta Mater., 36 (1997), 633-638.

57. B. Appolaire et al., “Free Growth of Equiaxed Crystals Settling in Undercooled $NH_4Cl$-$H_2O$ Melts,” Acta Mater., 46 (1998), 5851-5862.

58. A.A. Wheeler, W.J. Boettinger and G.B. McFadden, “Phase-Field Model for Isothermal Phase Transitions in Binary Alloys,” Phys. Rev. A, 45 (1992), 7424.

59. R. Kobayashi, “Modeling and Numerical Simulations of Dendritic Crystal Growth,” Physica D, 63 (1993), 410.

60. A. Karma and W.J. Rappel, “Quantitative Phase-Field Modeling of Dendritic Growth in Two and Three Dimensions,” Phys. Rev. E, 57 (1998), 4323.

61. C. Beckermann et al., “Modeling of Melt Convection in Phase-Field Simulations of Solidification,” J. Computational Physics, 154 (1999), 468-496.

62. X. Tong, C. Beckermann and A. Karma, “Velocity and Shape Selection of Dendritic Crystals in a Forced Flow,” Phys. Rev. E, 61 (2000), R49-R52.

63. H.J. Diepers, C. Beckermann and I. Steinbach, “Simulation of Convection and Ripening in a Binary Alloy Mush Using the Phase-Field Method,” Acta Mater., 47 (1999), 3663-3678.